

# Residual stress in polycrystalline thin Cr films deposited on fused silica substrates

ZP Mudau<sup>1</sup>, ARE Prinsloo<sup>1</sup>, CJ Sheppard<sup>1</sup>, AM Venter<sup>2</sup>, TP Ntsoane<sup>2</sup> and EE Fullerton<sup>3</sup>

<sup>1</sup>Department of Physics, University of Johannesburg, PO Box 524, Auckland Park, 2006, South Africa

<sup>2</sup>Research and Development Division, Necsa Limited, P.O. Box 582, Pretoria 0001, South Africa

<sup>3</sup>Center for Magnetic Recording Research, University of California, San Diego, 9500 Gilman Dr., La Jolla, CA 92093-0401, USA

Author e-mail address: cjsheppard@uj.ac.za

**Abstract.** The Néel temperature in thin film Cr coatings is strongly influenced by dimensionality effects, as well as strain and stress. In an investigation of Cr thin films, with thickness ( $t$ ) varied between 20 and 320 nm, deposited on fused silica substrates, the  $T_N$  values obtained from resistivity measurements indicate an increase with thickness as expected. This study is now extended to investigations of the in-plane stresses in these thin films, using specialised x-ray diffraction  $\sin^2\psi$ -method. The in-plane residual strain ( $\varepsilon$ ) present in the coating is determined from the slope of a linear plot through the fractional change in the lattice plane spacing (or Bragg peak position) versus  $\sin^2\psi$  plots. Residual stress ( $\sigma$ ) are calculated from the  $\varepsilon$  versus  $\sin^2\psi$  data by incorporation of the elastic properties of the coating material. The results indicate tensile stresses in all the samples.

## 1. Introduction

Cr is an archetypical antiferromagnet which forms an incommensurate spin-density-wave (SDW) structure that results from the nesting of the Fermi surfaces [1]. The magnetic transition temperature of bulk Cr is 311 K and has been found to be influenced by applied pressure [1, 2]. For polycrystalline Cr thin films deposited on fused silica substrates by the direct current magnetron sputtering method, a recent study has shown the  $T_N$  to be higher than in bulk material and that the  $T_N$  increases with the coating thickness ( $t$ ) [3].

Residual stress in thin films can be present as a result of the deposition and annealing techniques used [4]. Stress in thin films is classified as intrinsic and extrinsic [4, 5]. Intrinsic stress is caused by: i) presence of impurities; ii) voids; iii) partial growth; and v) re-crystallization during deposition [4]. Extrinsic stresses originate from differences in coefficient of thermal expansion (CTE) between the coating and the substrates [4]. The deposition parameters such as evaporation rate, geometry, temperature, and argon sputtering pressure, or impurities in the deposition system can also affect the stress values in both types of stresses [4].

Strain is the fundamental materials parameter that is measured by various techniques [6] based on destructive and non-destructive approaches. In the destructive approaches, strain relaxation is introduced by cutting/slitting actions with the residual strain that existed prior to this action inferred from the extent of the relaxation. The relaxation can be measured by mechanical strain gauges, or laser and optical based dilatometry techniques. Most non-destructive approaches are diffraction based of which x-ray diffraction is most generally used. With this technique, the spacing between atomic planes as an built-in material strain gauge is accurately measured [7]. Stresses are then calculated from the measured strains by incorporation of the elastic properties of the material.

In the x-ray diffraction method the lattice plane spacing,  $d_{hkl}$ , is precisely determined for a crystallographic reflection  $hkl$ , from the angular-position  $\theta$  of the measured diffraction peak by application of Bragg's law of diffraction. The lattice plane spacing  $d_{hkl} \equiv d_{\phi\psi}$  of crystallites orientated perpendicular to the diffraction vector  $\mathbf{L}_{\phi\psi}$ , as shown in the geometry of figure 1, is measured at various tilt angles  $\psi$  (source/tube geometry always fulfilling the Bragg condition for that reflection). The vector  $\mathbf{L}_{\phi\psi}$  along which the strain is measured bisects the angle between the incident and diffracted beam paths. The strain,  $\varepsilon_{\phi\psi}$ , in the Cr film along  $\mathbf{L}_{\phi\psi}$  is defined by [7]:

$$\varepsilon_{\phi\psi} = \frac{d_{\phi\psi} - d_0}{d_0}, \quad (1)$$

where  $d_0$  is the lattice plane spacing in an unstrained Cr thin film. In general defining  $\mathbf{L}_{\phi\psi}$  as one of the coordinate axis in figure 1, the strain in the Cr film's coordinates system ( $\mathbf{S}_i$ ) can be expressed in terms of  $\mathbf{L}_{\phi\psi}$  through a second-rank tensor transformation [7]:

$$\varepsilon_{ii} = a_{ik} a_{il} \varepsilon_{kl}, \quad (2)$$

where  $\varepsilon_{ii}$  is defined along  $\mathbf{L}_{\phi\psi}$  and  $i$  is usually set to three by substituting the appropriated direction cosines to  $a_{ik}$  and  $a_{il}$  in the form of  $\phi$  and  $\psi$ ,  $\varepsilon_{ii}$  can then be written as (in terms of direction cosines):

$$\begin{aligned} \varepsilon_{\phi\psi} = & \varepsilon_{11} \cos^2 \phi \sin^2 \psi + \varepsilon_{12} \sin 2\phi \sin^2 \psi + \varepsilon_{22} \sin^2 \phi \sin^2 \psi \\ & - \varepsilon_{33} \sin^2 \psi + \varepsilon_{33} + \varepsilon_{13} \cos \phi \sin 2\psi + \varepsilon_{23} \sin \phi \sin 2\psi. \end{aligned} \quad (3)$$

Equation (3) has six unknown variables that can be solved from at least six, but preferably more, independent measurements. Thus  $\varepsilon_{ii}$  can be solved in the Cr coordinate system ( $\mathbf{S}_i$ ) [4]. Generally, penetration depth of x-rays into Cr is about 10  $\mu\text{m}$  [8], thus the stress is measured in the surface region of the material only and a biaxial stress condition exists with components  $\mathbf{S}_1$  and  $\mathbf{S}_2$  in the plane of the material with no stress existing perpendicular to the free surface. For this biaxial stress condition it is further assumed that the material is single-phased, randomised crystallite orientations (no texture) and that the grain sizes are substantially smaller than the X-ray gauge volume. Equation (3) can then be simplified to be [5, 7]:

$$\varepsilon_{\phi\psi} = \left( \frac{1+\nu}{E} \right) \sigma_{\phi} \sin^2 \psi - \left( \frac{\nu}{E} \right) (\sigma_{11} + \sigma_{22}), \quad (4)$$

where  $\sigma_{\phi}$  is the stress in the surface direction  $\mathbf{S}_{\phi}$  shown in Figure 1,  $E$  is the Young modulus and  $\nu$  is the Poisson ratio,  $\sigma_{11}$  and  $\sigma_{22}$  are the principal stress components along  $\mathbf{S}_1$  and  $\mathbf{S}_2$  (shown in figure 1) on the surface of the film.

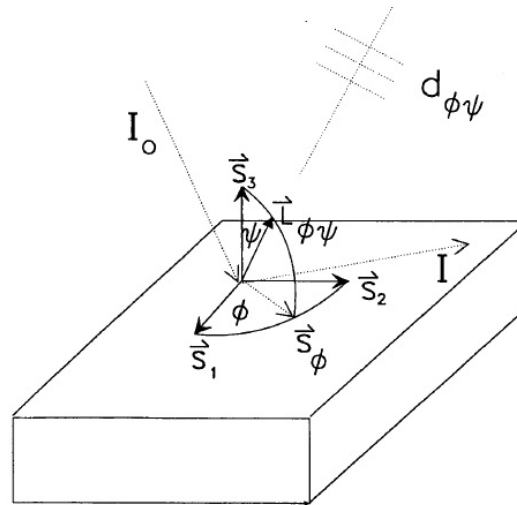


**Figure 1:** Schematic diagram defining the coordinates system of the sample  $S_1$  and the diffraction directions. The diffracted beam  $I$ , the incident beam  $I_0$  and the normal diffracting planes  $L_{\phi\psi}$  lie in the same vertical plane [4].

It is possible to solve the elastic constants empirically, however, the unstrained lattice  $d_0$  value is usually not known. Since  $E \gg (\sigma_{11} + \sigma_{22})$  the value of  $d_0$  may be replaced by  $d_{\phi_0}$ , i.e. the value measured at  $\psi = 0^\circ$  (perpendicular to the surface). This holds only for the biaxial stress condition applied here. This renders an error of about 0.1% and the values for  $\sigma_\phi$ ,  $\sigma_{11}$  and  $\sigma_{22}$  can be determined within this accuracy. This method thus becomes a differential technique not requiring standard references for calibration of the stress-free lattice spacing [9].

In this paper measurements and results are reported of the strains and stresses in Cr thin films deposited on fused silica substrates. The strains in the thin films were determined using the x-ray diffraction  $\sin^2\psi$  technique introduced above.

## 2. Experimental

The Cr films were prepared using direct current (DC) magnetron sputtering. The films were deposited at a substrate temperature and argon pressure of 973 K and 3 mT, respectively onto fused silica substrates (size: 10 mm<sup>2</sup> and thicknesses of 0.5 mm). The film thicknesses varied between 20 and 320 nm and were controlled by the deposition times. X-ray diffraction measurements were done on a Bruker D8 Discover diffractometer equipped with a Vantec 500 area detector. The source radiation was Cu  $K_\alpha$  set at 40 kV and 40 mA in conjunction with a monochromated incident beam 0.8 mm in diameter. The traditional  $\sin^2\psi$  method was used to study the residual strain in the material [4]. In strain analyses, changes in the lattice plane spacing are very small (typically  $10^{-4}$ ) which are achieved by selecting reflections with  $2\theta$  values larger than  $100^\circ$ . In the case of the Cr polycrystalline films the (310) reflection at  $2\theta$ -position  $115^\circ$  was used. Due to the penetration depth of the x-ray beam compared to the coating thickness, the measured strains are averaged through the coating thickness.

## 3. Results

The fused silica substrates are amorphous and thus do not contribute any coherent diffraction peaks to the diffraction patterns. In figure 2(a) the measured  $2\theta_{(310)}$  peak as function of the tilt angle,  $\psi$ , is shown for a Cr layer thickness of 160 nm.

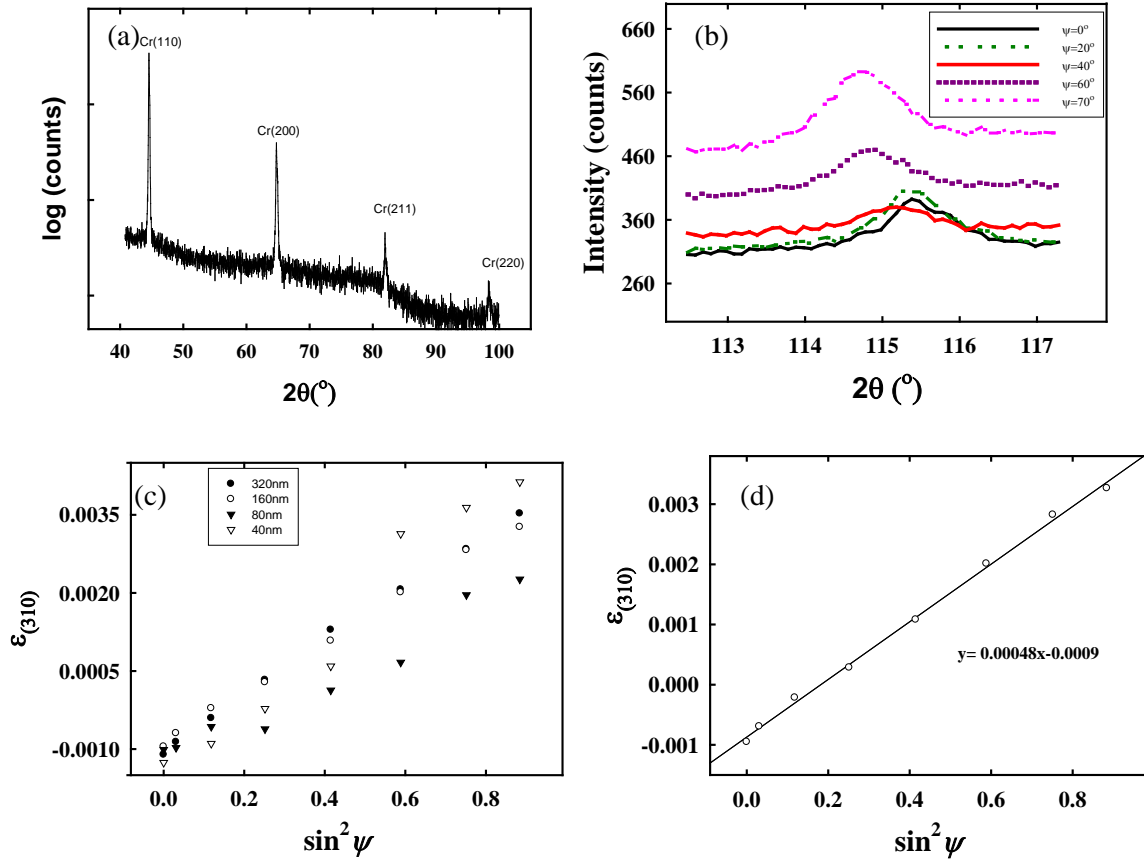


**Figure 2:** (a)  $\theta$ - $2\theta$  XRD of the film, for Cr film prepared on fused silica of  $t = 320$  nm. (b)  $2\theta_{(310)}$  Bragg peak of Cr as function of the tilt angle,  $\psi$ , measured on the 160 nm Cr film. (c) Plots of strain ( $\epsilon$ ) as function of  $\sin^2 \psi$  for different thicknesses of Cr coatings. (d) Strain ( $\epsilon$ ) versus  $\sin^2 \psi$  for the 160 nm sample showing the linear regression fit, where the gradient was used to calculate the residual stress.

It is clear that the central  $2\theta$ -position shifts to lower angles as  $\psi$  is increased from  $0^\circ$  to  $70^\circ$ . In figure 2(b) the strain,  $\epsilon_{(310)}$ , as function of  $\sin^2 \psi$  is shown for Cr layers with thickness ranging between 40 to 320 nm. At a Cr film thickness of 20 nm no (310) reflection could be observed due to the layer being very thin and not observable within the detection limit of the instrument. The positive slope in the  $\epsilon_{(310)}$  as function of  $\sin^2 \psi$  plots for all Cr film thicknesses indicates that the residual stress in the films are tensile [10] in all cases.

As an example of the typical data analysis procedure, a linear regression fit for  $\epsilon_{(310)} = \frac{d_{\phi\psi} - d_0}{d_0}$  as function of  $\sin^2 \psi$  for the 160 nm thin film is shown in figure 2(c). From equation (4) and assuming that  $\sin^2 \psi = 0$  at the intercept the unstrained lattice spacing  $d_0$  can be obtained from:

$$d_{\phi_0} = d_0 - \left(\frac{\nu}{E}\right)_{310} d_0 (\sigma_{11} + \sigma_{22}), \quad (5)$$

where the slope of the plot is given by:

$$\frac{\partial d_{\phi\psi}}{\partial \sin^2 \psi} = \left(\frac{1+\nu}{E}\right)_{310} \sigma_{\phi} d_0. \quad (6)$$

Using equations (5) and (6) the principal residual stress components  $\sigma_{11}$  and  $\sigma_{22}$  could be calculated. These values are summarized in table 1 and plotted as function of Cr film thickness in figure 3(a). The largest residual stress value is observed in the thinnest Cr coating, from where it decreases sharply to a value 966 MPa for the 80 nm coating followed by a gradual increase to values of 1179 MPa for the 160 nm coating and 1260 MPa for the 320 nm coating.

A qualitative description of the residual stress that develops in coated systems is given. The major contributor is cooling (thermal) stresses associated with the relative differences in their coefficients thermal expansion,  $\alpha$ , between the coating (c) and the substrate material (s). As the temperature decreases from the deposition temperature the following scenarios are possible [11]:

- $\alpha_c > \alpha_s$ : a tensile stress is generated in the coating,
- $\alpha_c = \alpha_s$ : no cooling stress will develop,
- $\alpha_c < \alpha_s$ : the resulting cooling stress is compressive.

Since the coefficient of thermal expansion of Cr is larger than that of the fused silica, when the system is cooled from the deposition temperature the Cr will contract more than fused silica, and because of the substantially larger volume of substrate material present, this causes tensile thermal stress [4] in the thin coating. Because the stress values are averaged over the film thicknesses, the result of figure 3(a) indicates that the stresses are influenced by two competing mechanisms: i) the film thickness; ii) the CTE differences. The interactive stress due to the first mechanism is dominant for thicknesses smaller than 80 nm.

Figure 3(b) shows the relationship between  $\sigma_{11}$  as a function of  $T_N$ , obtained previously [3]. There is an increase of the  $T_N$  with an increase in residual stress values for the samples with a thickness larger than 80 nm. The stress of the 40 nm sample is higher than that of the other samples in the series, this corresponds to an increase seen in the  $T_N$  value of the 40 nm sample [3]. It is evident that stress increases the  $T_N$  values of the samples series in correspondence to what is expected [2].

#### 4. Conclusions

The residual strain and stress analysis of Cr thin films coated on fused silica substrates, with thickness varying between 40 nm to 320 nm, was done using the x-ray diffraction  $\sin^2\psi$  technique. In general, the results reveal a large residual stress when the film is initially deposited, that drops off sharply with thickness, where after the stress values again increase more gradually for film thicknesses larger than 80 nm. As expected, the stresses remain tensile regardless of the film thickness due to the CTE differences between the film and substrate. Overall, there a link is observed between the  $T_N$  values and the residual stress values for samples that have thickness larger than 80 nm.

**Table 1:** Principal stress component results for Cr thin film thicknesses 40 nm to 320 nm deposited on fused silica substrates.

Thickness (nm)	Stress tensors (MPa)	
	$\sigma_{11}$	$\sigma_{22}$
40	1640 ± 128	1452 ± 129
80	966 ± 50	922 ± 50
160	1179 ± 18	1149 ± 18
320	1260 ± 18	1258 ± 18

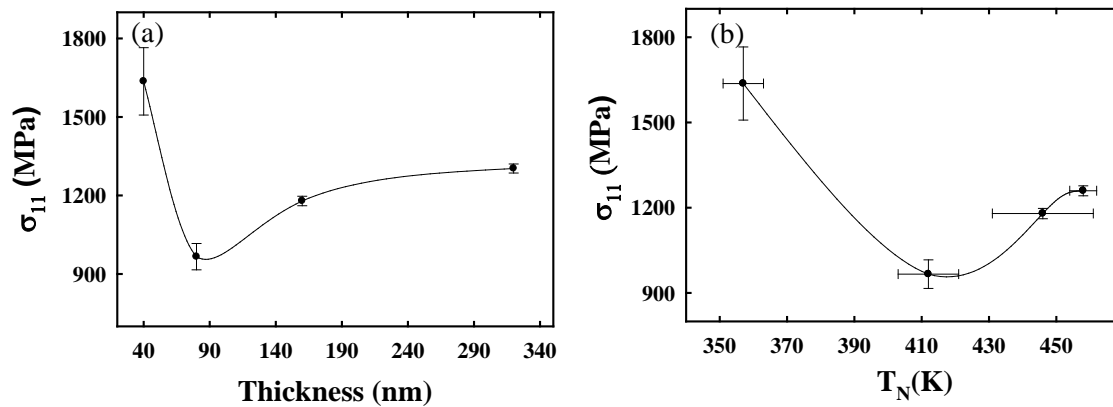


**Figure 3:** (a) Residual stress ( $\sigma_{11}$ ) versus Cr thin film thickness for coatings on fused silica. (b) Plot of residual stress ( $\sigma_{11}$ ) versus Néel temperature ( $T_N$ ). The solid lines in both figure (a) and (b) serve as guides to the eye to show trends.

## 5. Acknowledgement

The authors wish to thank the National Research Funding of South Africa for financial support towards this study (Grant number 80928 and 806260) and the Faculty of Science from the University of Johannesburg are acknowledged, as well as for the investment made under the National Equipment Programme (NEP, grant 60819) towards the procurement of the Discover instrument and Necsca for its operation and supervision in its use.

## References

- [1] Fawcett E, Alberts H L, Galkin V Y, Noakes D R and Yakhmi J V 1994 *Rev. Mod. Phys.* **66** 25
- [2] Zabel H 1999 *J. Phys. Condens. Matter* **11** 9303
- [3] Sheppard C J, Prinsloo A R E, Fernando R R, Mudau Z P, Venter A M and Fullerton E E 2013 *SAIP Conf. Proceedings* Submitted
- [4] Noyan I C, Huang T C and York B R 1995 *Crit. Rev. Solid State Mater.* **20** 125
- [5] Doerner M F and Brennan S 1988 *J. Appl. Phys.* **63** 126
- [6] Jian Lu 1996 *Handbook of measurement of residual stress*, Society for Experimental Mechanics Inc., Ed., The Fairmont Press Inc. ISBN 0-88173-229-X
- [7] Cullity B D 1978 *Elements of X-ray Diffraction* Massachusetts, Addison Wesley p447.
- [8] Van der Voort G and Friel J J 1996 *Developments in Materials Characterization Technologies*, ASM International, Materials Park, OH, p103.
- [9] Chiou S Y and Hwang B H 1998 *J. Phys. D: Appl. Phys.* **31** 349
- [10] Uchida H, Kiguchi T, Saiki A, Wakiya N, Ishizawa N, Shinozaki J and Mizuti N 1999 *J Ceramic Soc. Jpn.* **107** 606
- [11] Oladijo O P, Venter A M, Cornish L A and Sacks N 2012 *Surface and Coatings Tech.* **206** 4725